Proceedings of the 36th International Conference on Ocean, Offshore and Arctic Engineering
OMAE2017
June 25-30, 2017, Trondheim, Norway

OMAE2017-62498

REAL-TIME HYBRID MODEL TESTING OF A TOP TENSIONED RISER: A NUMERICAL CASE STUDY ON INTERFACE TIME-DELAYS AND TRUNCATION RATIO

Thomas Sauder[a,b] *
Asgeir J. Sørensen[a]
Kjell Larsen [c,a]

[a] Centre for Autonomous Marine Operations and Systems (NTNU AMOS), 7491 Trondheim, Norway
[b] SINTEF Ocean,† P.O. Box 4762 Sluppen, 7465 Trondheim, Norway
[c] Statoil ASA, Arkitekt Ebbells veg 10, 7053 Ranheim, Norway

ABSTRACT

This paper investigates the applicability of real-time hybrid model testing (ReaTHM testing) to the study of offshore systems in deep water. The focus is in particular on slender marine structures connecting floating structures to the seabed, and on how they could be truncated so that a model test setup at a reasonable scale could fit existing hydrodynamic laboratory infrastructures. In this context, ReaTHM testing consists in "substructuring" the slender structures in two parts. At the lower part of the water column, the first substructure is numerical, simulated using a nonlinear finite element method. On the upper part of the water column, the other substructure is physically modelled in an ocean basin. Both substructures interact in real-time through a set of sensors and actuators. This paper addresses through a case study the important issue of *accuracy* of ReaTHM testing, that is *how the behavior of the substructured system varies from that of the emulated system*. A top-tensioned riser in 1200m water depth is considered, with two truncation locations: 240m and 600m below the free surface. It is assumed that an artefact is introduced by the ReaTHM test setup, namely a time delay induced by e.g. the numerical calculations, or the actuation system. It is first shown how this artefact influences the accuracy of the setup, and then how the truncation ratio influences the tolerance of the ReaTHM test setup to such an artefact.

*Corresponding author (thomas.sauder@sintef.no)
†Earlier MARINTEK, SINTEF Ocean from 1st January 2017 through a merger internally in the SINTEF Group

1 INTRODUCTION

Hydrodynamic model testing serves several purposes, including the validation of numerical models, the study of complex physical phenomena, and final design verification. In this latter case, an ocean structure such as a floating production platform, is modelled at reduced scale, and exposed to the wave, wind and current conditions it may experience during its design life. It is typically verified that the motions of the platform, and the loads in the mooring and riser systems are acceptable under these environmental conditions. The test campaign is in general also a final risk mitigation campaign, during which extreme events, such as green water on deck, wave impact, or riser/mooring/structure collision could be detected, prior to making any major investment decision.

Oil and gas exploitation is however taking place at steadily increasing water depths: the company Shell just set a new record in September 2016, when their disconnectable FPSO started to exploit the Stones field (Gulf of Mexico) in 2900m water depth [1]. Let us assume that such a system should be tested in an ocean basin, and let h be the water depth. An estimate of the *radius* of the mooring system footprint is $1.0h$-$1.7h$ for a taut mooring system, and $1.5h$-$2.5h$ for a catenary mooring system [2, 3, 4]. From these values, and the characteristic dimensions of the floating structure, an estimate of the required basin dimensions can be obtained. Inserting numbers, it becomes clear that modeling such systems at a reasonably large scale (λ >1/100), in any of the existing ocean basin laboratories is not feasible. This is due

to both the vertical extent of the mooring/riser system, but also due to its horizontal footprint.

The challenges associated to deep-water model testing have been addressed in [5] and various solutions have been suggested, among others ultra-small scale testing, or outdoor testing. The state-of-the-art approach to solve such problems, is based on *passive truncation* of the slender marine structures, which will be discussed in more detail in Section 2.

One envisioned solution is to perform real-time hybrid model testing (abbreviated ReaTHM® testing[1] in the following), and more specifically for this problem: *active truncation*. This means that the floating structure and the upper part of the slender structure system are modelled physically in the laboratory, while its lower part, connected to the seabed infrastructure, is *simulated* on a computer. In practice, these two so-called *substructures* may interact as follows. The force from the lower end of the physical substructure (floater and upper part of the riser) is measured, and applied as a top force on the numerical substructure (lower part of the riser). The resulting displacement of the numerical substructure is then calculated, and applied to the bottom part of the physical substructure using underwater actuators. In reality, this coupling is not perfect: various *artefacts*, related to measurement errors, noise, time delay or jitter induced by the numerical calculations, limited bandwidth of the actuators, among others, may appear. These artefacts make the *substructured system* deviate from the *emulated* system, that is our best representation of reality.

It is of crucial importance to evaluate to which extent such artefacts influence the accuracy of a ReaTHM test setup. On the one hand, if, for a given accuracy target, the requirements on the control system, including sensors, control algorithms and actuation system, are beyond what is technically feasible, one will conclude that ReaTHM testing is unfeasible for the considered setup. On the other hand, when the ReaTHM test setup is feasible and realized, end-users of the test results are to be provided with quantitative estimates of the accuracy of these results. While uncertainty quantification in classical model testing has received considerable attention, see e.g. [6], ReaTHM testing is a new field of research in which this aspect has not been much focused on yet.

The present paper consists of a case study, aimed at illustrating this point. A top-tensioned riser in 1200m water depth is studied, with two truncation locations: 240m and 600m below the free surface. One type of artefact is considered, namely the time delay induced by e.g. numerical calculations. It is investigated how this time delay influences the behaviour of the substructured system as compared to the emulated system. The paper is organized as follows. Section 2 provides a short review of deep-water model testing, and truncation techniques. Section 3 and 4 describe the method used in the present case study and the numerical results. Conclusions are summarized in Section 5.

[1] ReaTHM® testing is a registered trademark of SINTEF Ocean AS.

2 PREVIOUS WORK

The challenges related to model testing of deep-water systems have been discussed in [5]: existing laboratory infrastructure may not have the horizontal extent nor the water depth required to accommodate ultra-deep water systems, while outdoor testing and ultra-small scale testing do not allow for an accurate modelling of the floating system and for a controlled environmental loading. The state-of-the-art approach for the verification of ultra-deep water systems involves a numerical study in addition to model testing, and is therefore called "hybrid verification" [7].

Statically-equivalent truncated systems, and hybrid verification. Hybrid verification is founded on the fact that the dynamic behaviour of marine slender structures is well-described by validated numerical codes such as RIFLEX [8], while free surface hydrodynamics including wave-current-body interaction still requires experiments. Hybrid verification is a three-step procedure.

Step (1). First, model tests are performed using a (passive) truncated version of the mooring and riser system. The truncation is performed in order to achieve *static* similarity between the truncated and full-depth systems. The design of the truncated system is very dependent on the type of system under study. The process involves in general an architectural design phase during which the truncation point and a first estimate of line properties, possibly clump weights, or blocking springs are decided upon. The parameters of the truncated system are then refined by solving an optimization problem [9,10,11], whose objective function is a measure of the difference between the static characteristic of the full-depth and truncated systems. The constraints of the optimization problem can be related to the manufacturability and integrity of the truncated system. For example, the yield strength of coil springs should not be exceeded [9].

Model testing is performed with this statically-equivalent truncated system, which ensures that the floating structure behaves *similarly to* the full-depth system when exposed to the environmental loads. It is important to emphasize that the *dynamic* tension in the mooring and riser lines measured during these model tests, cannot be used directly for design verification: indeed, inertial loads and transverse drag loads on the truncated slender marine structures are in general significantly less than on the full-depth system, which causes discrepancies on the dynamic tension, especially in harsh sea-states. For the same reason, designing a truncated system which is *dynamically*-equivalent over a wide range of sea-states, is a difficult task. We will come back to this.

Step (2). The second stage of hybrid verification involves establishing a numerical model of the truncated setup, and the calibration of the hydrodynamic model of the floating system in order to match model test results [7]. Wave drift loads, wave-current interaction and viscous damping of the floater are parameters that are in general tuned in this phase.

Step (3). When satisfactory agreement with model tests is achieved, the numerical results are "extrapolated": the truncated mooring/riser system is replaced by the full-depth system, and simulations are run in relevant environmental conditions to obtain dynamic line tensions, extreme excursions of the floater, which are used to verify the design.

The hybrid verification is considered as the most reliable verification method as of today, but its main weakness lies in the execution time of the model test, calibration and extrapolation phases.

Dynamically-equivalent truncated systems. During the last years, researchers have therefore attempted to design truncated setups exhibiting a correct *dynamic* behaviour, which would remove the need for post-calibration and numerical extrapolation.

Starting from a statically-equivalent system, Ferreira et al. [12] suggested to achieve dynamic equivalence by jointly varying the diameter and mass of the segments, while keeping the submerged weight constant, and the static properties of the system unchanged. Based on a numerical case study, they concluded that the truncated setup was able to replicate the dynamic line tensions in sea-states with comparable strength to the ones used in the calibration. When quite different sea-states were investigated, motions of the floater could however deviate significantly. No detailed results were reported regarding dynamic line tensions in these sea-states. Using a similar approach, Wei et al. [13] presented a step-wise, systematic and efficient way of solving the optimization problem mentioned in the previous paragraph. Dynamic equivalence was only verified for quite mild sea-states, very close in terms of strength to the ones used in the optimization process. An *overspecialization* of the dynamically-equivalent system is therefore likely to be an issue with both approaches. Note that they also require nonlinear time domain simulations to be performed prior to the test. This may prevent the method to be applied in a commercial setting, for which, in general, only a short period of time is available to design and manufacture the truncated system.

Following another approach, Argyros [4] studied the drag-induced decay of transverse vibrations of a taut string, subjected to top motions. Based on this, he defined a truncation length as the minimum length below which the line could be assumed to be vibrating in air with regards to its in-plane normal vibrations, in other words, a point below which drag-induced damping and added mass would have an insignificant effect on the transverse motions. To model the lower, truncated, part of the line, a nonlinear (polynomial) spring is used at the truncation point, as well as a dashpot acting transversely to the line. An additional axial force, calibrated from numerical simulations at full-depth, may be added when studying extreme sea states. Argyros' work allows for a rapid assessment of dynamic processes related to taut lines in deep water, such as drag-induced damping of their transverse vibrations, reflection and transmission due to impedance mismatch and shackle-induced damping, when segment with different properties, as chains and polyester segments, are connected. However, while the method seems very adequate for the truncation of a large class of taut polyester mooring systems in deep water, it cannot be applied directly to other classes of slender marine structures, such as steel catenary risers. Also, even though the boundary conditions at the truncation point look quite simple (polynomial stiffness, transverse dashpot, and additional axial force), it may be unpractical to realize them with simple components as springs or dashpots during model tests.

Active methods and ReaTHM testing Some researchers have investigated the feasibility of active truncation, in which the truncated part of the system is simulated using e.g. a nonlinear finite element method (FEM). The connection between the physical and numerical substructures happens through a set of sensors and actuators [14, 15, 16]. In that setting, dynamic similarity is achieved intrinsically, and the challenges lie in the practical implementation of the method. One important difficulty resides in the fact that when Froude scaling is applied, time runs $\lambda^{-\frac{1}{2}}$ faster than full-scale real-time, which sets quite stringent requirements on the efficiency of the numerical model. Christiansen [17] proposed using neural networks, trained by nonlinear FEM, to solve this issue. These "active" approaches have never been applied in a commercial setting for the study of floating systems in ultra-deep water. However, Vilsen et al. [18] showed promising results for this application by performing ReaTHM tests, in which twelve mooring lines were fully truncated, and simulated with RIFLEX [8] running twelve times faster than real-time. The same research group successfully performed ReaTHM testing of a floating wind turbine [19, 20]. In that case, the wind-induced loading was simulated, and applied in real-time on a physical model of the wind turbine. The physical model was located in the Ocean Basin at SINTEF Ocean, and was also subjected to (physical) waves and current. The system ran in closed loop, i.e. the measured motions of the floating wind turbine were used in the calculation of the aerodynamic loading. Even if the application of ReaTHM testing was different, many practical aspects were also relevant to model testing of ultra-deep water systems.

It is out of the scope of the present paper to provide a thorough literature review of real-time hybrid testing in general, and its applications. The interested reader may consult [19], and references therein, for an introduction. Also, the work of Drazin et al. [21] and of Terkovics et al. [22] is of direct relevance to the topic addressed here, i.e substructuring of top tensioned risers, and possible accuracy issues. They investigated the so-called *substructurability* of beams, and accuracy losses induced by imperfections at the physical-numerical interface. Also, the present work is an extension of the approach used by Bachynski et al. [23] for the design of the above-mentioned ReaTHM tests of the floating wind turbine.

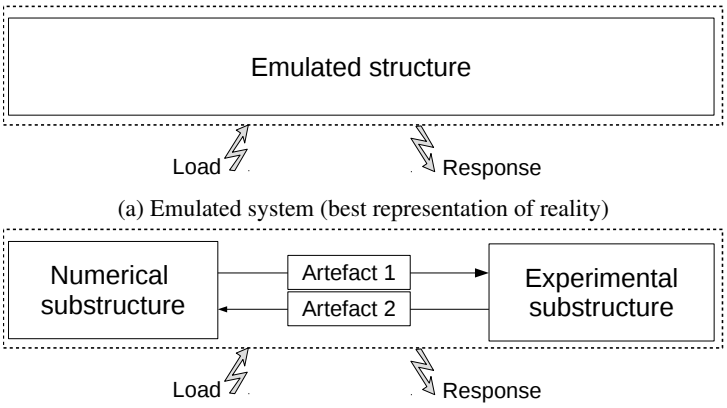

(a) Emulated system (best representation of reality)

(b) Substructured system, and artefacts introduced by the control system. In the present case study, Artefact 1 corresponds to a time delay, induced by the computation and actuation. Artefact 2 is not modelled, i.e. the connection is considered ideal.

FIGURE 1: The emulated system and the substructured systems including artefacts.

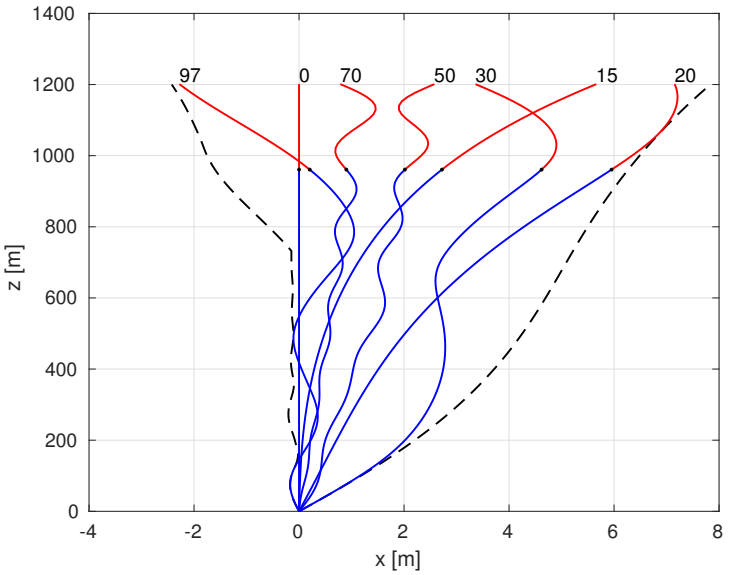

FIGURE 2: The solid curves represent the riser's configuration at given time instants. Here $\alpha = 0.8$, the numerical substructure is represented in blue, and the physical substructure in red. The dashed lines represent the envelope of the riser motions when subjected to the dynamic load case (100 s), see Figure 3.

3 METHOD

The suggested general approach to study the accuracy of a ReaTHM test setup consists in comparing the response of the emulated system (Fig. 1a) subjected to a given relevant load case, with the response of the substructured system including artefacts (Fig. 1b) to the same load. This is described in details in the following procedure, and each point will be detailed in the next paragraphs.

1. Define the emulated system (Fig. 1a)
2. Partition the system into a physical substructure and a numerical substructure (Fig. 1b)
3. Choose a relevant load case containing amplitudes, frequencies, events of interest
4. Set up a high-fidelity model of the physical substructure
5. Perform co-simulation of the substructured system (Fig. 1b), including time delay or other artefacts
6. Define a quantity of interest (QoI) in terms of the response
7. Calculate the error y on the QoI, between the emulated and substructured/imperfect systems
8. Define an admissible upper bound of the error, and deduce the specifications of the ReaTHM test setup

Emulated and substructured systems In the present case study, the emulated system is a 1200m long top-tensioned steel riser with a circular cross-section, an outer diameter of 300 mm and a wall thickness of 15 mm. The steel density is 7850kg/m^3, the material is assumed elastic with a Young modulus of 206 GPa. The fluid transported in the riser has a density of 800 kg/m^3, and the sea-water a density of 1025 kg/m^3. A vertical top tension of 3 MN is applied.

In order to accomodate it in an ocean basin, the riser is truncated. The *truncation ratio* is defined as

$$\alpha = 1 - \frac{\text{truncation depth}}{\text{total depth}} = \frac{\text{numerical depth}}{\text{total depth}}$$

According to this definition, a truncation ratio $\alpha = 0$ means no truncation (purely physical riser), and $\alpha = 1$ means that the riser is fully represented by numerical simulations. Two truncation ratio are investigated here: $\alpha = 0.5$ and $\alpha = 0.8$, corresponding to truncation points located 600m and 240m below the free surface, respectively. The curve indexed "0" in Figure 2 shows the static equilibrium configuration for $\alpha = 0.8$. Assuming that the ReaTHM tests are performed using Froude scaling with a scale factor of $\lambda = 1/100$, $\alpha = 0.5$ corresponds then to a truncation depth of 6m, representative of combined wave and current tests in a 10m deep wave tank using a movable bottom allowing for current recirculation. The truncation ratio $\alpha = 0.8$ would be applicable for tests performed at a larger scale, or in greater water depths.

An analysis such as presented by Argyros [4] can give a sense of the dynamics of the riser at the truncation point. Inserting numbers corresponding to the present problems, it can be estimated that the amplitude of the transverse vibrations of the riser have almost halved at the truncation point when $\alpha = 0.8$ ($l_{50} \approx 286$ m).

Load case Depending on the focus of the model tests, the system under study will be exposed to various types of environmental loads, most likely various combinations of wind, current and wave loads. The latter type is focused on here. Waves can induce various types of loading in the slender structure system, ranging from monochromatic or narrow banded spectra to impulsive loads, when extreme events occur. The load case selected for the evaluation of the ReaTHM test setup (point 3 in the above procedure) should cover the type of loading that is expected during the test. In the present case, a frequency sweep (chirp) covering the frequency range $[0, 0.5]$ Hz was applied as a horizontal force on the top of the riser, see Figure 3. This load case provides a rather simple indicator of the bandwidth of the system in the linear wave excitation range, for transverse vibrations of the riser. If impulsive loads were of interest, approximations of Dirac or Heaviside type of signals could be chosen. If compression of the riser, or axial-transverse coupling due to curvature or tension modulation were to be studied, the load would also include a vertical component.

A specialized FE code The problem at hand requires a *numerical* solution of the riser's dynamics to evaluate the response of the emulated and substructured systems to an arbitrary load. Ideally, a Finite Element (FE) software for global analysis of slender marine structures such as RIFLEX [8] should be used. However, at the time this study was performed, there was no ready solution to include the artefacts depicted in Figure 1b in the solution process. A customized FE code was therefore developed for this purpose. A bar element formulation, similar to that presented in [24], was used, including drag and effective weight loads. The boundary conditions for the riser were *fixed*, i.e. prescribed displacements, at the bottom, and *free*, i.e. prescribed loads, at the top. The static analysis was performed using Newton-Raphson iterations and accounts for geometric nonlinearities. The mass, damping and stiffness matrices obtained at the static equilibrium were used in a *linear* dynamic simulation. A 4^{th} order Runge-Kutta scheme with adaptive step size was used for the time integration. Note that in general, and in particular for e.g. steel catenary risers, a nonlinear dynamic analysis should be performed, to account for geometric nonlinearities and structure-soil interaction.

Two FE models were set up, representing the physical and the numerical substructures, respectively. The top of the latter was connected to the bottom of the former. n_{el} elements were uniformly distributed along the riser's length: the physical substructure included $\lceil (1-\alpha) n_{el} \rceil$ elements, and the numerical substructure $\lfloor \alpha n_{el} \rfloor$ elements. It was verified that the QoI were converging when increasing n_{el}, see Figure 7 on page 10. Satisfactory convergence was obtained for 60 elements, for which the error measure associated to all quantities of interest (which will be defined later on in this Section) were less than 2% . This value of $n_{el} = 60$ was used from this point.

Co-simulation with artefacts The above-mentioned convergence study was also performed on the substructured system. The coupling between the numerical substructure and the physical substructure was then assumed to be perfect, in the sense that the top displacement of the bottom part of the riser was matching exactly the bottom displacement of the top part of the riser. In addition to this *kinematic* compatibility condition, a *dynamic* compatibility condition was satisfied at the truncation point, at every *synchronization time step* Δt. Note that, as indicated previously, the inner time step of time integration of each substructure was adapted according to its own dynamics.

However, the main objective of the present study was to study the effect of an *imperfect* coupling. To this purpose, an `artefact` class was developed, that allowed modelling various types of artefacts such as time delays, jitter (i.e. varying time delay), and noise. An illustration of the possible effect of this class is provided in Figure 4. Only constant time delays were of interest in the present study

The system was then subjected to an external load $\tau(t)$. In our case study, τ consists of the top force variation only, but it could also have been generated by variations of the ambient current velocity. Let $\tau_1(t)$ be the part of τ applied to the physical substructure, and $\tau_2(t)$ be the part of τ load applied to the numerical substructure. Let f be the force and d the displacement at the interface between the substructures. Let $\bar{f}$ and $\bar{d}$ be their "imperfect" counterparts. At each synchronization time step Δt, the following iterative procedure ensures force- and displacement-consistency between the substructures.

1. At the initial iteration, assume no change at the interface, that is $\bar{f}(t+\Delta t) = \bar{f}(t)$, and $\bar{d}(t+\Delta t) = \bar{d}(t)$.
2. Perform time integration of the numerical substructure between t and $t+\Delta t$, with interface force varying from $\bar{f}(t)$ to $\bar{f}(t+\Delta t)$, and external load from $\tau_2(t)$ to $\tau_2(t+dt)$.
3. Evaluate $d(t+\Delta t)$ from the response of the numerical substructure
4. Evaluate $\bar{d}(t+\Delta t)$ from $d(t'), t' \in [0, t+\Delta t]$ and the artefact (here a simple time delay)
5. Perform time integration on the physical substructure between t and $t+\Delta t$, with interface displacement varying from $\bar{d}(t)$ to $\bar{d}(t+\Delta t)$, and external load from $\tau_1(t)$ to $\tau_1(t+dt)$.
6. Evaluate $f(t+\Delta t)$ from the response of physical substructure
7. Evaluate $\bar{f}(t+\Delta t)$ from $f(t'), t' \in [0, t+\Delta t]$ and the selected artefact (here: none, but another time delay, or some noise could be added)
8. Repeat from 2 until convergence of $\bar{f}(t+\Delta t)$ and $\bar{d}(t+\Delta t)$, advance time, and restart from step 1.

Note that this procedure reduces to a classical coupled analysis when no imperfection is included, that is when $f(t) \equiv \bar{f}$ and $d \equiv \bar{d}$. In the context of our study, a synchronization time step of $\Delta t = 10$ms was chosen. It was verified that the solution was insensitive to Δt for values less than 50ms. This conclusion is of course specific to the present system.

Response of interest and error indicator As indicated earlier, the objective is to *compare the response* of the emulated and the (imperfect) substructured systems when subjected to the same

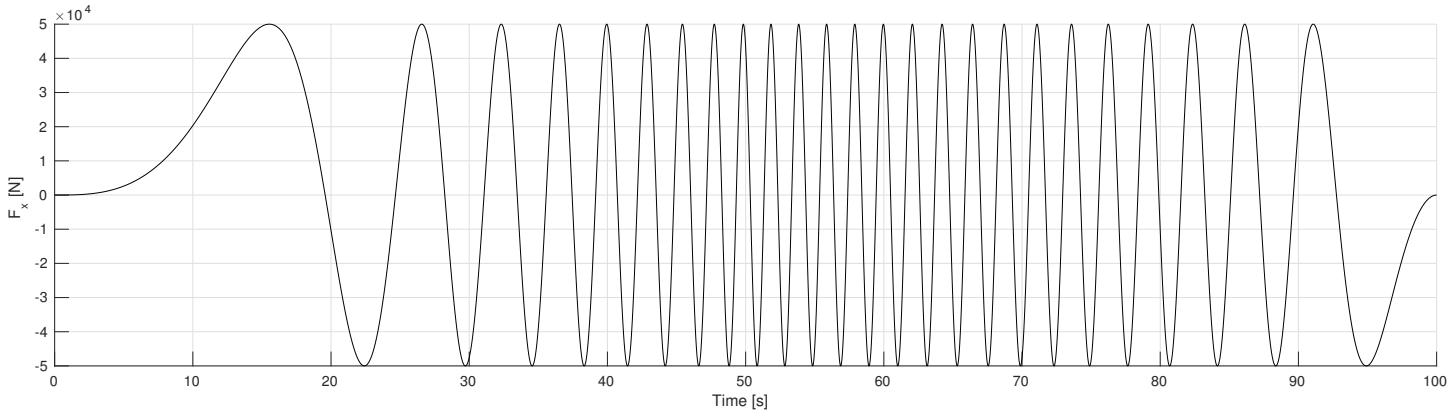

FIGURE 3: Time series of the frequency sweep.

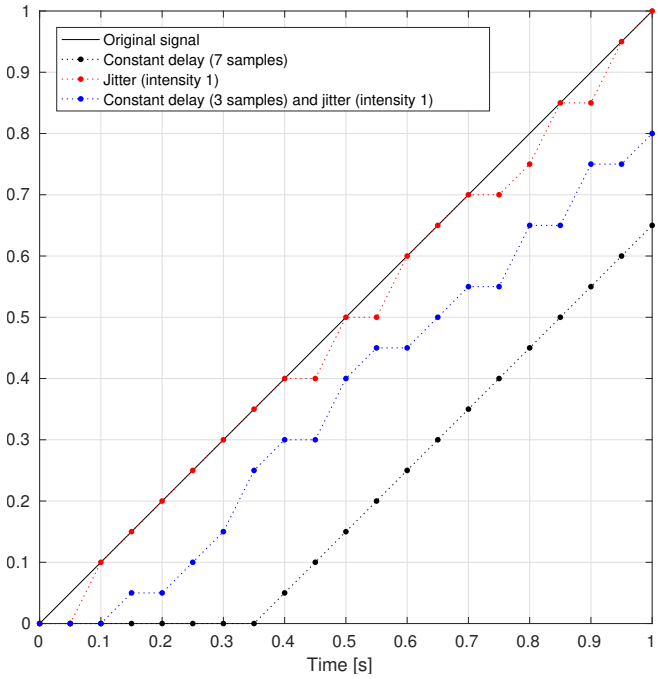

FIGURE 4: Illustration of a delayed and jittered (dimensionless) signals, as simulated by the `artefact` class. In this illustration, the sampling frequency is 20Hz.

load. To do so, it is necessary to define a Quantity of Interest (QoI) characterizing the response, as well as an error measure allowing to compare the QoIs. In the studied case, the riser was subjected to the horizontal force loading, and the impedance of the system was of interest, so we chose to look in particular at the following response time series:

1. horizontal velocity of the top of the riser (main indicator),
2. instantaneous power at the top of the riser,
3. top position at the top of the riser,
4. force time series at the bottom of the riser.

For each Quantity of Interest (QoI), an L^2-based indicator of the error between the emulated and the imperfect substructured system was considered:

$$y(s, s_{ref}) = \frac{1}{2}\log_{10}\frac{\int_0^T \left(s - s_{ref}\right)^2 dt}{\int_0^T \left(s_{ref}\right)^2 dt} \tag{1}$$

where s_{ref} is the reference signal, corresponding to the QoI of the emulated system, and s corresponds to its counterpart, originating from the imperfect substructured system. T is the duration of the load signal, equal here to 100s. If for example, discrepancies of maximum 1% are tolerated between s and s_{ref}, then y should not exceed -2.

Other examples of QoI include the maximum/minimum values of a given response component, or other statistical quantities such as mean value or standard deviation. Note that interface-related indicators, such as the incompatibility of the force at the truncation point, are good indicators of the performance of the control system as such, but are not of direct interest for the outcome of the test.

Note also that the present approach relates to the *accuracy* of the ReaTHM test setup, but also covers the *stability* of such a closed-loop system: the fact that the system becomes unstable will in general lead to a significant loss of accuracy.

4 NUMERICAL RESULTS

The method outlined in the previous Section was applied to the 1200m riser test case, subjected to the load depicted in Figure 3 . We focused in particular on the two following issues.

1. For the case $\alpha = 0.8$, we investigated the effect of the delay induced by computation/actuation, ranging from 150ms to 750ms full-scale. This corresponds to a 15 to 75ms range at model scale for $\lambda = 1/100$.
2. The effect of the truncation ratio ($\alpha = 0.8 \rightarrow 0.5$) on the sensitivity to the time delay.

Sensitivity to the time delay (for $\alpha = 0.8$) The delay induced by the computation/actuation phase was studied. Figures 8 to 10, in the Appendix, show the time series of the horizontal velocity, power and horizontal position of the top node, respectively, for various values of the delay. These values originate from the physical substructure. Figure 11 shows the time series of the horizontal component of the bottom force, which comes from the numerical substructure.

It can be seen from Figures 8 and 9 that the top node velocity, and thus the dissipated power are quite sensitive to the time delay, especially in the middle part of the time series, where the frequency content is close to 0.5Hz. This shows the limitations in terms of bandwidth of the ReaTHM test setup when a too large time delay is present.

The sensitivity of the top node position (Fig. 10) and of the bottom node force (Fig. 11) to the time delay is less significant. For the former, this is due to the fact the integration from velocity to position over one cycle tends to make discrepancies less apparent, with the selected error measure. For the latter, this is due to the weak coupling of the bottom horizontal force, at 1200m water depth, and the dynamic horizontal load 240m below the free surface.

For each Quantity of Interest (QoI), the error indicator y was calculated from equation (1). The results are presented in Figure 5. Note that y decreases when the length of the bar increases, and note the logarithm in the expression of y. From this Figure, it can for instance be decided that the delay should be less than 150ms full-scale (i.e. 15ms at scale 1:100) to ensure an error of less than 5% on the power estimation.

Influence of the truncation ratio ($\alpha = 0.8 \rightarrow 0.5$) The next step was to investigate how this result evolves when the truncation point was lowered from 240m to 600m below the free surface. Figure 6 shows the error indicators corresponding to the latter case ($\alpha = 0.5$). These indicators can be compared with Figure 5.

The only error indicator that increases when the truncation ratio decreases is $y_{Fx,bottom}$. Yet, this increase is not significant. However, a significant reduction of the other indicators, related to the top node, is observed when going from $\alpha = 0.8$ to $\alpha = 0.5$. Indeed, even with a 750ms delay (75ms at model scale), the power estimated from the imperfect substructured system was within 5% of the target, obtained from the emulated system. Comparing directly the time series in Figure 12 shows indeed little sensitivity of the horizontal velocity to the time delay, when $\alpha = 0.5$.

It can be concluded that the "bandwidth" of the ReaTHM test setup is significantly improved by decreasing α. Intuitively, this is explained by the fact that the coupling between the response of top of the riser and dynamics of the truncation point becomes weaker when the distance between these two points increases. Therefore, an artefact at the truncation point will have less influence on the response of the upper part of the system,

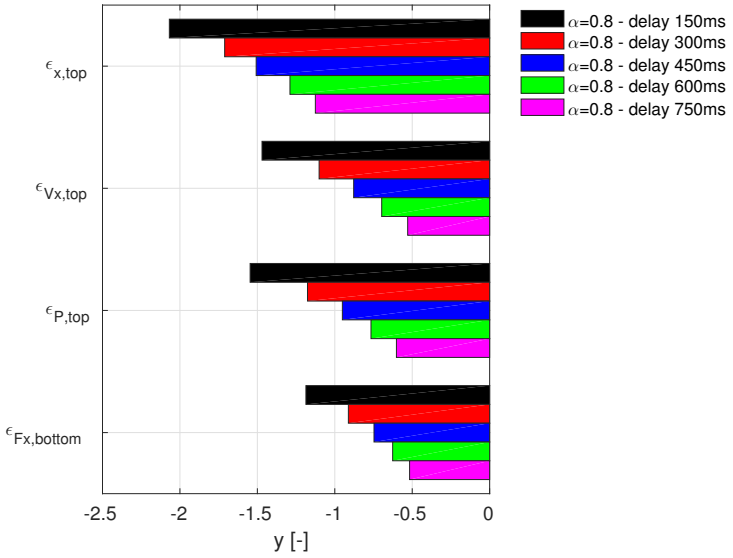

FIGURE 5: Influence on a time delay induced by e.g. calculation time or actuation, on various error indicators y. From top to bottom: error on the horizontal position of the top node, on the horizontal velocity, on the dissipated power, and on the horizontal force at the bottom node. The truncation ratio is $\alpha = 0.8$.

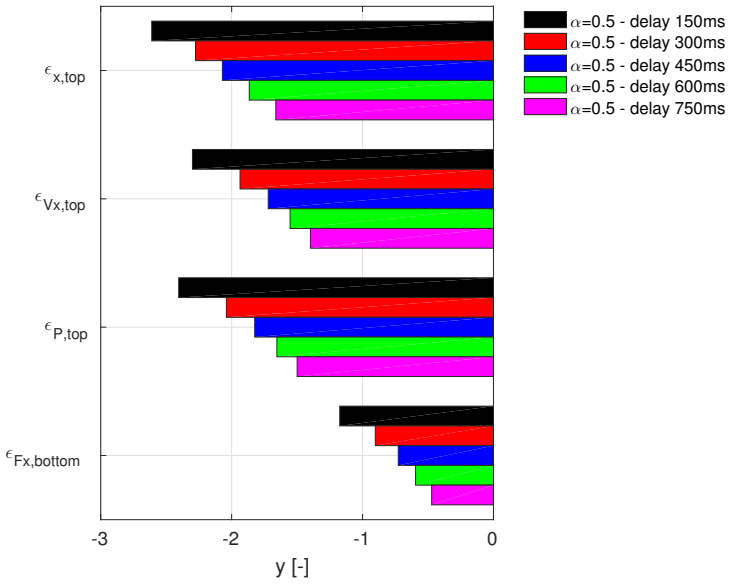

FIGURE 6: Similar to Figure 5, but with $\alpha = 0.5$.

and on the related QoI. This conclusion would of course not hold if the force at the *lower* end of the riser was the focus.

5 CONCLUSION

In the present paper, a numerical case study was performed to evaluate the *accuracy* of a ReaTHM test setup involving a truncated top tensioned riser. The accuracy was defined through a set of Quantities of Interest (QoI) and an error indicator y. Using this measure, the emulated system (best available model of the physical system under study), and the substructured system, involving artefacts, could be compared. It was emphasized that the QoI should not necessarily be related to the *interface* between the numerical and physical substructures (as force or displacement incompatibility indicators would be), but to the physical values of interest and to the very purpose the ReaTHM test.

For illustration purposes, a 1200 m long top-tensioned riser was truncated, or "substructured". Two truncation ratios were investigated: $\alpha = 0.5$ and $\alpha = 0.8$. The physical substructure consisted on the upper part of the riser. Its bottom end was displacement-controlled, based on numerical simulation of the lower part of the riser, which was the numerical substructure. An artefact, namely a time delay, was artificially introduced at the truncation point to represent a possible delay induced by the calculation or actuation phase.

On the one hand, for a relatively large truncation ratio, it was shown that this delay had a great influence on most of the selected QoI, and that an upper limit value for the delay could be obtained to meet a given accuracy target. It was then shown that the influence of the time delay could be significantly reduced by redefining the truncation point. In other words, the constraints on the ReaTHM test setup were significantly relaxed if the truncation point was moved further away from the locations of interest, i.e. at a greater water depth. In this case, the requirements on numerical simulations would also be relaxed (the spatial extent to simulate would be less), but the needed water depth and footprint on the basin floor would increase. These conclusions are summarized in a qualitative way in Table 1. Note that the result of this case study is of course specific to the level of coupling and damping present in the studied system, and to the selected set of QoI.

Open issues and further work In the present work, the time delay was the only type of artefact that was modelled. This choice was based on previous experience, showing that time delays, inevitable in such setups, may have severe consequences on the accuracy. However, other types of artefacts are present, such as noise from sensors, jitter due to nonlinear iterations or buffers, scaling due to calibration errors, and disturbances from actuators. Their combined effect, and possible interaction should be studied.

The object of the case study was a top-tensioned riser in zero current, and only transverse oscillations of the riser were considered. The conclusion of the study would most probably be very different if more coupling between the axial and transverse motions was present, such as in a steel catenary riser, or a tension leg platform's tendon in extreme seas. Such structures should be part of the scope of a further study. A *nonlinear dynamic* analysis is required to describe their behaviour in a satisfactory manner.

TABLE 1: Comparison of the two truncation ratios. A plus (resp. minus) sign means tougher (resp. milder) requirements.

Requirements on the:	$\alpha = 0.5$	$\alpha = 0.8$
- control system (incl. actuators)	-	+
- laboratory infrastructure	+	-
- numerical simulation tool	-	+

When studying more complex structures, combined artefacts, and possibly more complex load cases, the computational cost of each co-simulation is expected to increase. In that case, it is important to minimize the number of co-simulations, while ensuring a reliable estimation of the "limit state" of the ReaTHM test setup, i.e. the amount of imperfection leading to an unacceptable loss of accuracy. It should also be possible to confirm which *type* of artefact has the greater consequence on the accuracy, in order to focus on this aspect in the design of the ReaTHM test setup. These aspects are focused on in ongoing research.

ACKNOWLEDGMENTS

This work was supported by the Research Council of Norway through the Centres of Excellence funding scheme, Project number 223254 - AMOS, and through the project 254845/O80 Real-Time Hybrid Model Testing for Extreme Marine Environments.

REFERENCES

[1] Bowers, S., 2016. "Shell begins production at world's deepest underwater oilfield". *The Guardian*, Sept.

[2] the ITTC Specialist Committee on Deep Water Mooring, 1998. Final Report and Recommendations to the 22nd ITTC. Tech. rep.

[3] Chakrabarti, S. K., ed., 2005. *Handbook of Offshore Engineering.* Elsevier. OCLC: 835766876.

[4] Argyros, A., 2011. "Efficient Dynamic Modelling of Deepwater Moorings". Phd thesis, University of Cambridge.

[5] Stansberg, C. T., Ormberg, H., and Oritsland, O., 2002. "Challenges in Deep Water Experiments: Hybrid Approach". *Journal of Offshore Mechanics and Arctic Engineering,* ***124***(2), Jan., p. 90.

[6] Qiu, W., Sales Junior, J., Lee, D., Lie, H., Magarovskii, V., Mikami, T., Rousset, J.-M., Sphaier, S., Tao, L., and Wang, X., 2014. "Uncertainties related to predictions of loads and responses for ocean and offshore structures". *Ocean Engineering,* ***86***, Aug., pp. 58–67.

[7] Baarholm, R., Fylling, I., Stansberg, C. T., and Oritsland, O., 2006. "Model testing of ultra-deepwater floater systems: Truncation and software verification methodology". In ASME 2006 25th International Conference on Ocean, Offshore and Arctic Engineering.

[8] MARINTEK, 2016. RIFLEX 4.8.0 Theory Manual.

[9] Fylling, I., and Stansberg, C. T., 2005. "Model Testing of Deepwater Floating Production Systems: Strategy for Truncation of Moorings and Risers". In DOT Brazil.

[10] Molins, C., Trubat, P., Gironella, X., and Campos, A., 2015. "Design Optimization for a Truncated Catenary Mooring System for Scale Model Test". *Journal of Marine Science and Engineering,* ***3***(4), Nov., pp. 1362–1381.

[11] Felix-Gonzalez, I., and Mercier, R. S., 2016. "Optimized design of statically equivalent mooring systems". *Ocean Engineering,* ***111***, Jan., pp. 384–397.

[12] Ferreira, F. M., Lages, E. N., Afonso, S. M., and Lyra, P. R., 2016. "Dynamic design optimization of an equivalent truncated mooring system". *Ocean Engineering,* ***122***, Aug., pp. 186–201.

[13] Wei, H., Xiao, L., Tian, X., and Kou, Y., 2017. "Four-level screening method for multi-variable truncation design of deepwater mooring system". *Marine Structures,* ***51***, Jan., pp. 40–64.

[14] Buchner, B., Wichers, J. E. W., De Wilde, J. J., and others, 1999. "Features of the State-of-the-art Deepwater Offshore Basin". In Offshore Technology Conference, Offshore Technology Conference.

[15] Watts, S., 2000. "Simulation of Metocean Dynamics: Extension of the Hybrid Modelling Technique to Include Additional Environmenal Factors".

[16] Cao, Y., and Tahchiev, G., 2013. "A Study on an Active Hybrid Decomposed Mooring System for Model Testing in Ocean Basin for Offshore Platforms". In ASME 2013 32nd International Conference on Ocean, Offshore and Arctic Engineering, American Society of Mechanical Engineers.

[17] Christiansen, N. H., Voie, P. E. T., and Høgsberg, J., 2015. "Artificial Neural Networks for Reducing Computational Effort in Active Truncated Model Testing of Mooring Lines". In OMAE2015-42162.

[18] Vilsen, S., Sauder, T., and Sørensen, A. J., 2017. "Real-time hybrid model testing of moored floating structures using nonlinear finite element simulations". the Society of Experimental Mechanics.

[19] Sauder, T., Chabaud, V., Thys, M., Bachynski, E. E., and Sæther, L. O., 2016. "Real-time Hybrid Model Testing of a Braceless Semi-submersible Wind turbine. Part I: The Hybrid Approach". In ASME 2016 35th International Conference on Ocean, Offshore and Arctic Engineering, No OMAE2016-54435.

[20] Chabaud, V., 2016. "Real-time hybrid model testing of floating wind turbines". PhD thesis, Norwegian University of Science and Technology.

[21] Drazin, P. L., Govindjee, S., and Mosalam, K. M., 2015. "Hybrid Simulation Theory for Continuous Beams". *Journal of Engineering Mechanics,* ***141***(7), July, p. 04015005.

[22] Terkovics, N., Neild, S. A., Lowenberg, M., Szalai, R., and Krauskopf, B., 2016. "Substructurability: The effect of interface location on a real-time dynamic substructuring test". *Proceedings of the Royal Society A: Mathematical, Physical and Engineering Science,* ***472***(2192), Aug., p. 20160433.

[23] Bachynski, E. E., Chabaud, V., and Sauder, T., 2015. "Real-time Hybrid Model Testing of Floating Wind Turbines: Sensitivity to Limited Actuation". *Energy Procedia,* ***80***, pp. 2–12.

[24] Rustad, A. M., Larsen, C. M., and Sørensen, A. J., 2008. "FEM modelling and automatic control for collision prevention of top tensioned risers". *Marine Structures,* ***21***(1), Jan., pp. 80–112.

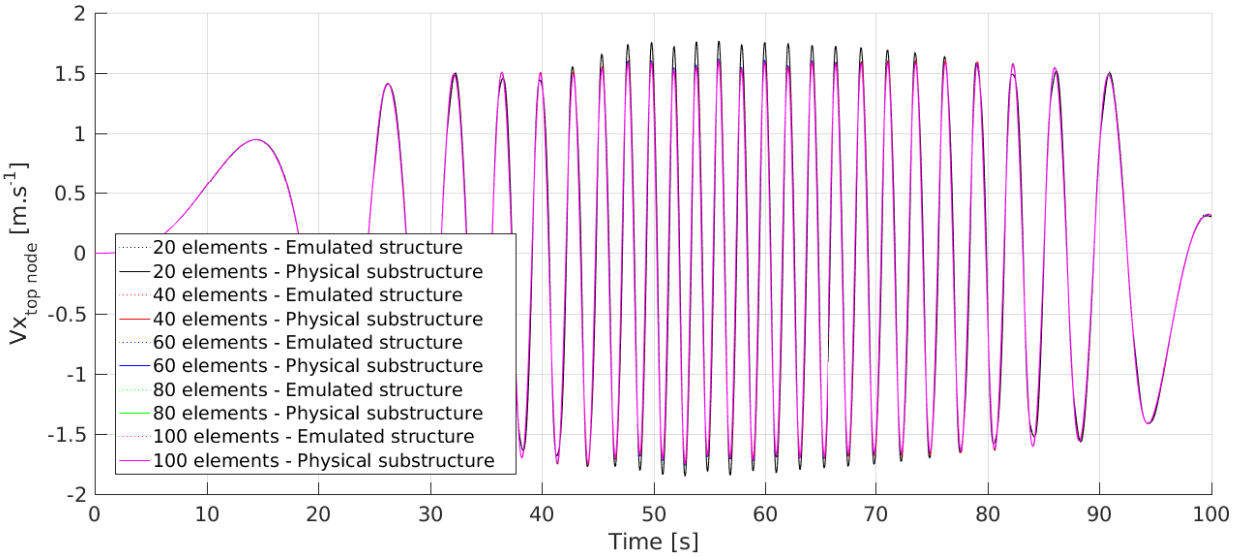

FIGURE 7: Influence of the number of elements of the emulated system n_{el} on the time series of the horizontal velocity at the top node. The number of elements of the physical substructure is $\lceil (1-\alpha) n_{el} \rceil$ with $\alpha = 0.5$ in the present case.

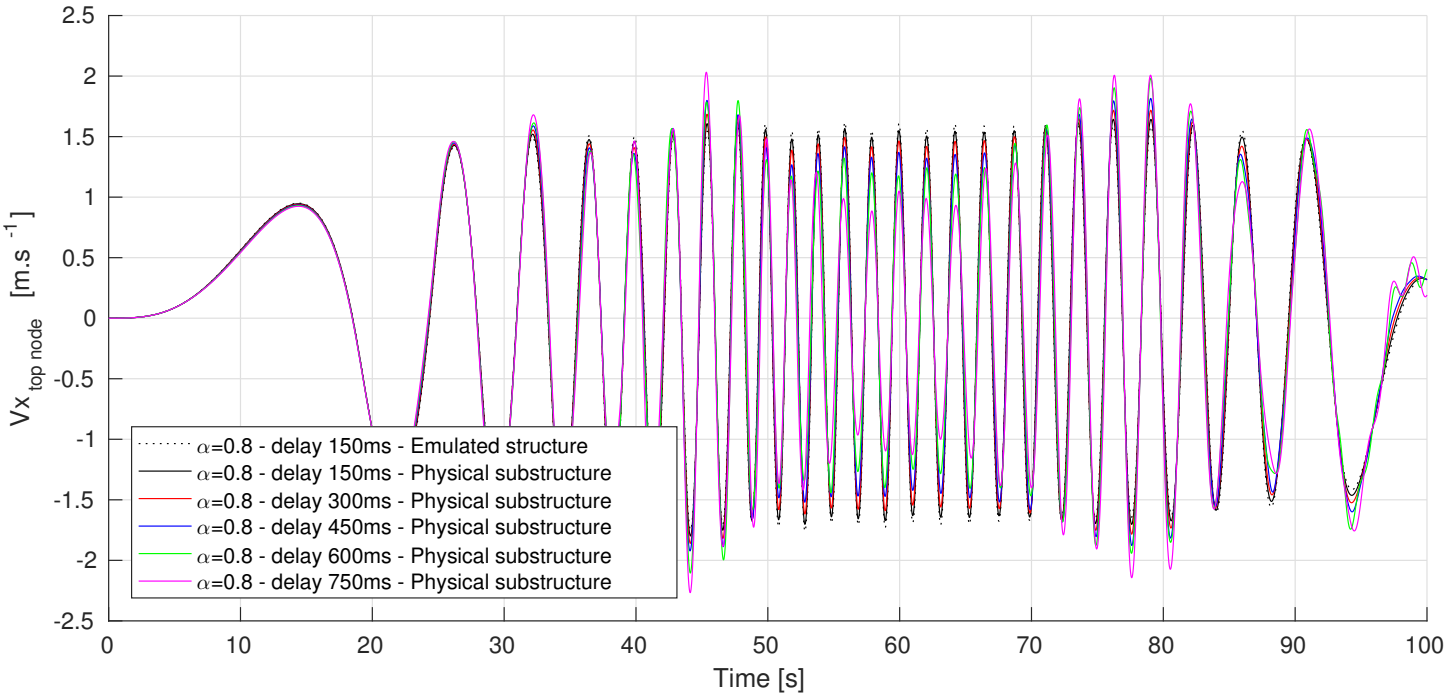

FIGURE 8: Influence of a time delay induced by e.g. the time integration of the numerical substructure, on the time series of the horizontal velocity at the top node. The truncation ratio is $\alpha = 0.8$.

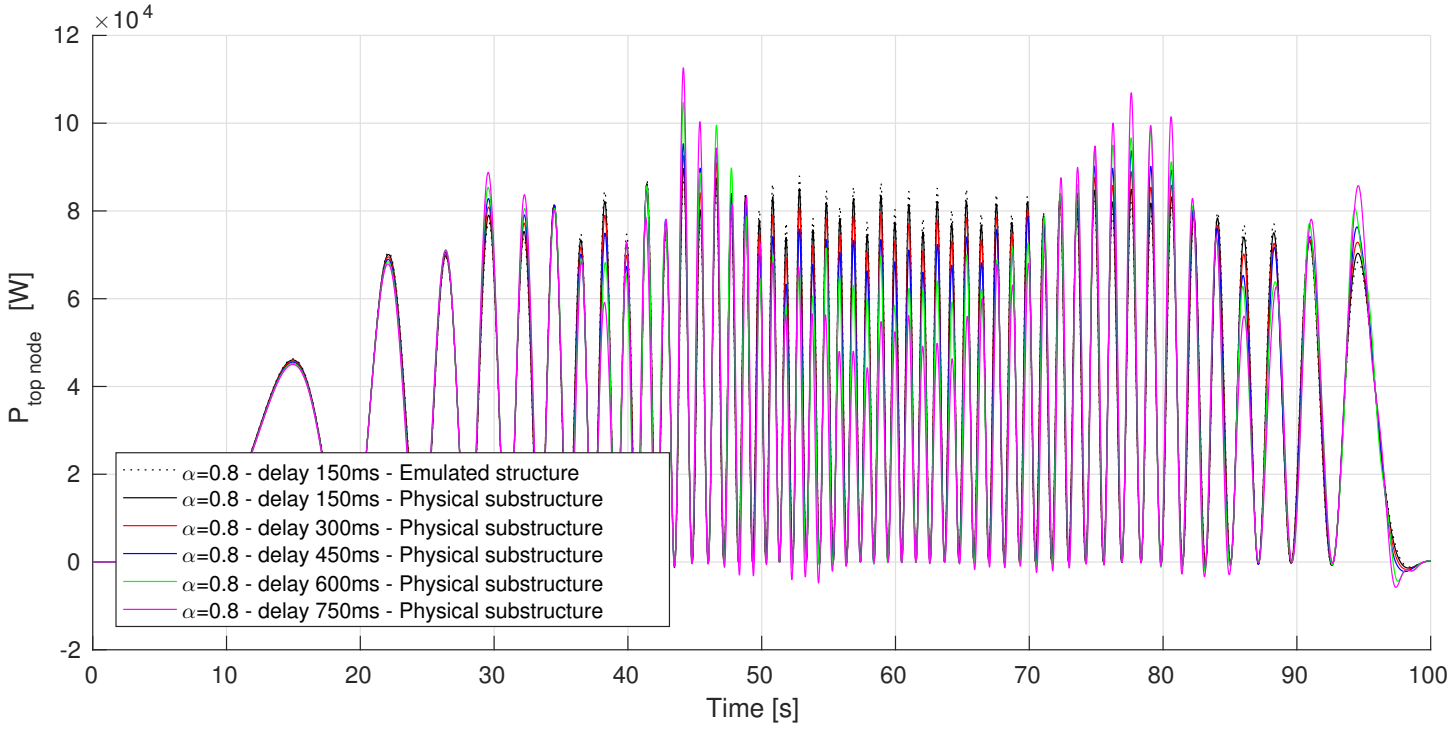

FIGURE 9: Influence of a time delay induced by e.g. the time integration of the numerical substructure, on the time series of the power at the top node. The truncation ratio is $\alpha = 0.8$.

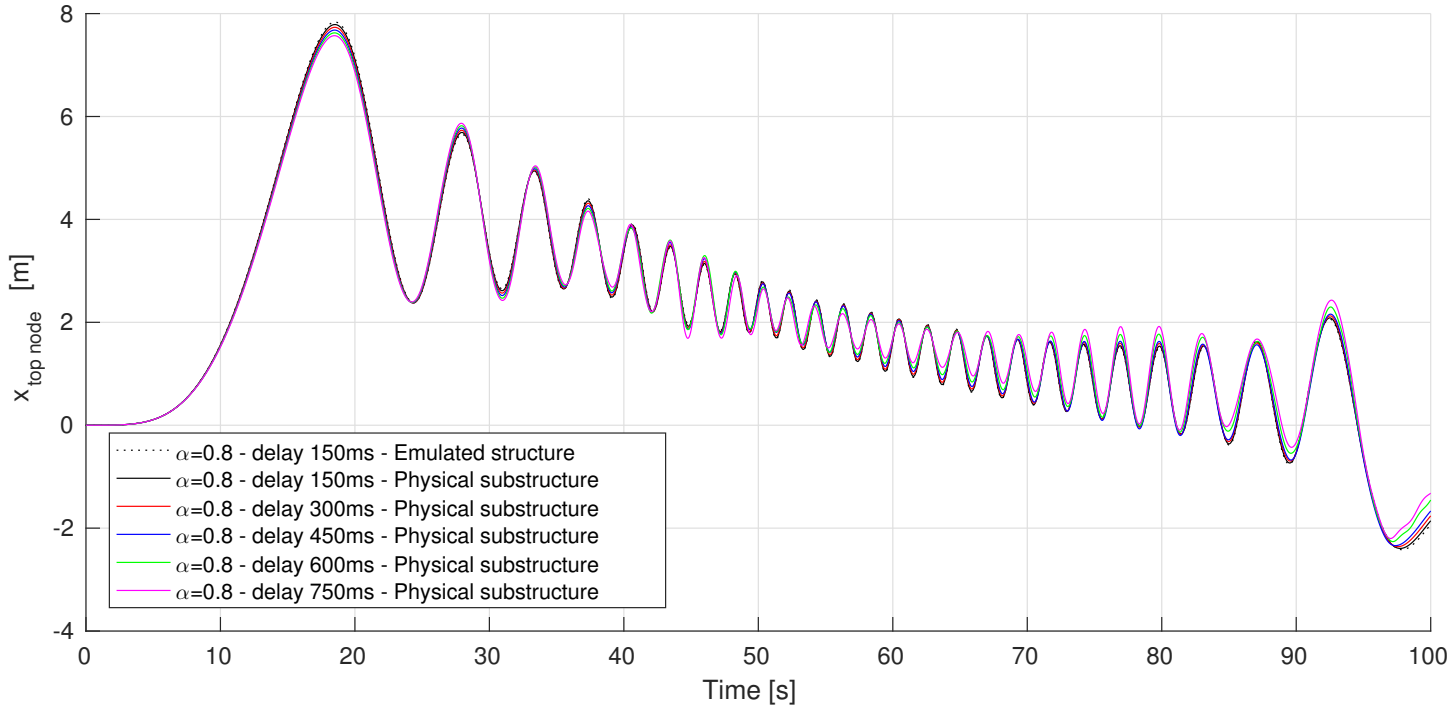

FIGURE 10: Influence of a time delay induced by e.g. the time integration of the numerical substructure, on the time series of the horizontal position of the top node. The truncation ratio is $\alpha = 0.8$.

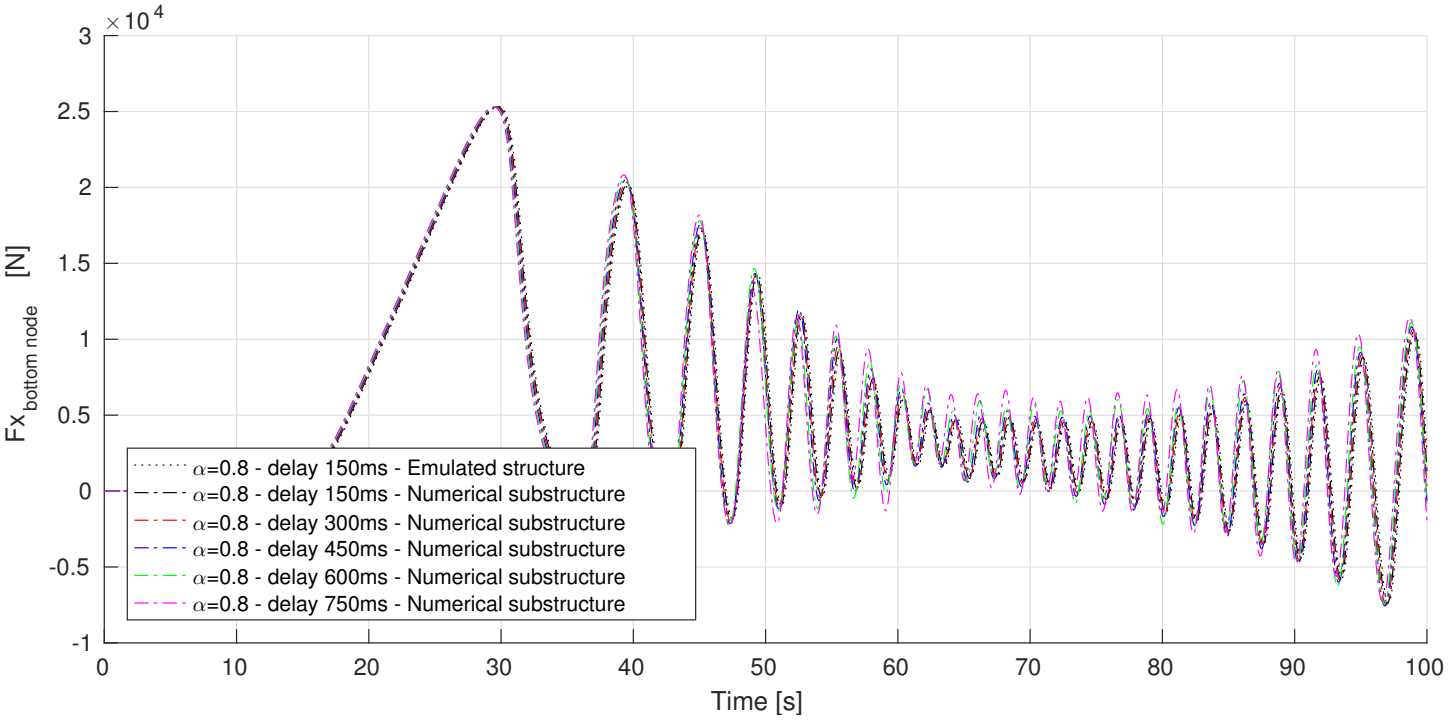

FIGURE 11: Influence of a time delay induced by e.g. the time integration of the numerical substructure, on the time series of the horizontal force at the bottom node. The truncation ratio is $\alpha = 0.8$.

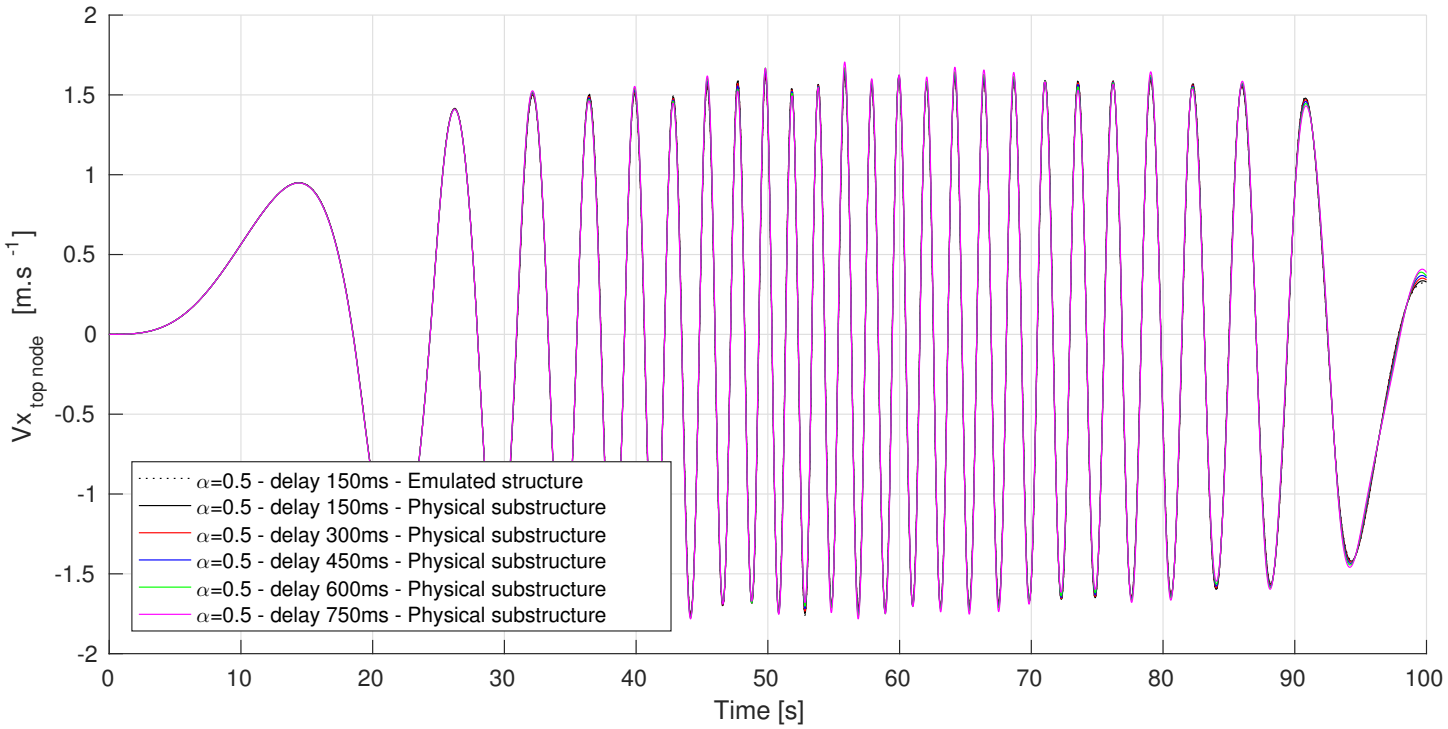

FIGURE 12: Similar to Figure 6, but with $\alpha = 0.5$.